Association of Sonic Hedgehog with the Extracellular Matrix Requires its Putative Zinc-Peptidase Activity

Carina Jägers and Henk Roelink
University of California, Berkeley, United States

Abstract

Sonic Hedgehog (Shh) has a catalytic cleft characteristic for zinc metallopeptidases. Nevertheless, the putative peptidase activity of Shh is dispensable for activation of the response in vitro and was deemed “pseudo-active”. Still, Shh has significant sequence similarities with some bacterial peptidoglycan metallopeptidases defining a subgroup within the M15A family that, besides having the characteristic zinc coordination domain, can bind two calcium ions. Extracellular matrix (ECM) components in animals include heparan-sulfate proteoglycans, which are analogs of bacterial peptidoglycan and thus potential peptidase substrates. We found that the putative metallopeptidase activity of Shh is required for its association with ECM as well as for non-cell autonomous signaling. The putative peptidase requires the presence of at least 0.1 μM zinc and is inhibited by mutations affecting critical catalytic residues as well as extracellular calcium. Our results indicate that Shh is a calcium-regulated zinc metallopeptidase.

Introduction

The *Hedgehog* (*Hh*) gene was first identified in the *Drosophila melanogaster* screen performed by Christiane Nüsslein-Volhard and Eric Wieshaus in the late 1970s (Nüsslein-Volhard and Wieshaus, 1980). Like other segment polarity genes found in this screen, *Hh* genes are widely conserved among animals, and mammals have three Hh paralogs (Sonic -, Indian -, and Desert Hedgehog) that play roles in development (Echelard et al., 1993). Like all other Hhs, Shh is synthesized as a pro-protein that undergoes autoproteolytic cleavage mediated by the C-terminal part yielding an N-terminal part (ShhN) that is the active ligand. Structural analysis of ShhN revealed its similarity to zinc-peptidases and Shh coordinates a zinc ion with residues H141, D148, and H183 (Hall et al., 1995). The notion that Shh signaled through a peptidase activity was quickly rejected by demonstrating that mutation of a critical residue involved in catalysis (E177) did not impair the ability of Shh to activate the Hh response (Fuse et al., 1999), and consequently the zinc coordination domain of Shh is often referred to as its “pseudo active” site (Bosanac et al., 2009; Maun et al., 2010). Still, a role for the putative catalytic activity is supported by the finding that Shh-E177A is unable to mediate non-cell autonomous signaling from the notochord to the overlying neural plate (Himmelstein et al., 2017). The ability of Shh-E177A to induce the Hh response when expressed ectopically in the developing brain could be explained by cell-autonomous signaling. Purified ShhN-E177A is reportedly more stable in solution than ShhN, supporting the notion that Shh has an intrinsic cannibalistic peptidase activity (Rebollido-Rios et al., 2014). Perhaps unsurprisingly, the zinc coordination domain is found mutated in some individuals with the Shh signaling-related birth defect holoprosencephaly (Roessler et al., 1996; Traiffort et al., 2004), further indicating that the putative peptidase activity of Shh is important for normal function. This is consistent with structures of Shh complexed with its receptor Patched1 (Ptch1), showing that the N-terminal 22 residues of Shh that are not part of the peptidase domain, mediate binding to Ptch1 (Gong et al., 2018; Qi et al., 2018a; 2018b) and suffice to regulate Ptch1 activity (Tukachinsky et al., 2016).

Some bacteria have genes coding for peptidases that coordinate zinc and calcium identically to Shh (Rebollido-Rios et al., 2014; Roelink, 2018). These bacterial peptidases (members of the M15A subfamily of zinc D-Ala-D-Ala carboxypeptidases) cleave murein peptidoglycans, suggesting that Shh too might cleave a glycan-modified protein, possibly a matrix heparan sulfate proteoglycan (HSPGs). Several HSPGs bind Shh and can both negatively and positively affect the Shh response (Capurro et al., 2008; Carrasco et al., 2005; Guo and Roelink, 2019; Witt et al., 2013). Furthermore, mutations in *Ext1* and *-2* coding for glycosyltransferases that catalyze glycosaminoglycan addition to the core proteins, disrupt Hh signaling in vertebrates (Guo and Roelink, 2019; Siekmann and Brand, 2005) and insects (Bellaiche et al., 1998). It is thus plausible that functional conservation between BacHhs and Shh is reflected in the ability of Shh to cleave proteoglycans, thereby affecting the Shh response and/or extracellular matrix (ECM) distribution, independent of its binding to the canonical Hh receptors.

Possible mechanisms of catalysis of zinc peptidases have been elucidated with the help of structural models of enzyme-inhibitor complexes. Thermolysin is a well-studied zinc metallopeptidase structurally related to Shh (Hall et al., 1995; Rebollido-Rios et al., 2014). Shh and Thermolysin coordinate zinc via two histidine and an aspartic acid residue. A catalytic glutamic acid residue initiates catalysis (E177 in mouse Shh) by accepting a proton from water to form the nucleophilic hydroxide that attacks the carbonyl carbon, further stabilized by the coordinated zinc. With the two stacking histidine (or occasionally tyrosine) residues a pentacoordinate transition state is formed and resolved into the hydrolyzation products (Matthews, 2002; Tronrud et al., 1992).

By mutating the residues critical for catalysis, we provide evidence that the putative peptidase activity of Shh is required for the association of ShhN to the ECM and for non-cell autonomous signaling. Release of Shh into the ECM is enhanced in the presence of μM amounts of zinc. The ECM-associated Shh is active in signaling, indicating that the putative peptidase activity of Shh mediates its release into the ECM to facilitate non-cell autonomous signaling.

Results.

A high degree of similarity to bacterial peptidoglycan peptidases indicates that Shh is catalytically active

ShhN homologs in bacteria share a conserved zinc coordination motif that defines a family of prokaryotic proteins characterized by the Hh/DD-peptidase fold. This peptidase fold is a central, five-stranded antiparallel β-sheet that separates the zinc coordination domain from several α-helices, as found in ShhN. (van Heijenoort, 2011) (Figure 1C). This zinc coordination motif is also found in Lysostaphin, a metallopeptidase that cleaves peptide bonds in peptidoglycan, and is referred to as the “LAS” (Lysostaphin, D-alanyl-D-alanine peptidase, Shh) arrangement (Bochtler et al., 2004). Both Lysostaphin and members of the M15A family of D-alanyl-D-alanine peptidases play critical roles in bacterial cell wall/biofilm modification through the cleavage of peptidoglycans (Rawlings and Barrett, 2013).

Several species of bacteria have a gene coding for a protein that has calcium and zinc coordination motifs very similar to that of Shh (Roelink, 2018). A 105 amino acid domain comprising these calcium and zinc coordination domains is up to 65% identical between Shh and such bacterial proteins (BacHhs). All residues involved in zinc and calcium coordination are conserved. While the zinc coordination domain is common in M15A peptidases, the combination of this domain with a calcium coordination motif is only found in Shh/BacHh (Figure 1A). No clear homologs of any of the Hh receptors can be identified in these bacteria, further supporting the idea that BacHhs serve as peptidases and not as ligands. The typical Hh fold can also be recognized in Hedglings (Fairclough et al., 2013) and in Hedglets. Hedglets, proteins of

unknown function that have one or two Hh domains are present in Lophotrochozoans, Cephalochordates and Echinoderms (sequences and accession numbers in supplemental file). The Hh-related sequences in Hedglings and Hedglets lack most residues typically required for catalysis and are more distantly related to Hhs/BacHhs. Principal component analysis (PCA) of Hhs, BacHhs, Hedglings, Hedglets, and other Hh-related bacterial M15A metallopeptidases peptidases shows tight grouping of Hhs with BacHs (Figure 1B). The typical arrangement of the calcium and zinc coordination domains (Figure 1C, D) defines the Hh/BacHh subfamily, while the relationship to other M15A peptidases is restricted to the zinc coordination domain. The remarkable similarly between Hhs and BacHhs supports the notion that they share a calcium-regulated metallopeptidase activity.

Peptidoglycans, the substrates for M15A metallopeptidases, are a major component of the bacterial periplasmic space/ECM and have some similarities to the proteoglycans that are common in extracellular matrix (ECM) of vertebrates, insects, and *cnidarians* (corals and jellyfish). Both bacterial cell wall peptidoglycans and matrix proteoglycans of animals are large molecules in which polypeptides are covalently attached to chains of glycans. We propose that functional conservation between BacHhs and Shh is reflected in the ability of Shh to catalytically modify ECM proteoglycans.

Active ShhN associates with the extracellular matrix

A conceivable function for the Shh peptidase could be the cleavage of a substrate allowing transition from a cell-bound to an ECM-bound state. We assessed ECM-bound Shh in the fraction of macromolecules that remain on the tissue culture plate after non-lysing cell removal. HEK293T cells were transfected with *Shh* (mutant) constructs and removed by washing with PBS and agitation. In order to exclude a role for Dispatched1 in the transition from a cell-bound to an ECM-bound state (Tian et al., 2005), we assessed the association of Shh-C199* (ShhN) with the ECM and found that ShhN could readily be detected in the ECM fraction using gel electrophoresis followed by SYPRO Ruby staining (Figure 2A). Visualizing Shh-C199* by staining of the decellularized plates with the anti-Shh mAb5E1, well-defined Shh “footprints” of Shh producing cells were observed (Figure 2B). Shh-C199* is commonly referred to as a “soluble” protein due to the absence of C-terminal cholesterol, however, the Shh “footprints” suggest that the protein leaves the cell and enters the adjacent ECM in a direct manner and not via an intermediate soluble form from the medium. Surprisingly, more Shh could be detected in the ECM than in the lysate of *Shh-C199** transfected HEK293T cells (Figure 2B), together showing that entry of ShhN into the ECM is robust and cumulative. Shh-responsive LightII cells plated on the decellularized and Shh-conditioned ECM showed that this fraction is able to elicit a transcriptional Hh pathway response similar to Shh-conditioned medium, a commonly used form of pathway activation (Figure 2C).

Mutations in the Zinc coordination domain reduce the stability of Shh-C199*

Mutating the residues directly involved in the coordination of zinc are obvious candidates to assess a role for the putative peptidase activity. However, Shh mutants in the zinc coordination domain could barely be detected the N-terminal processed form (ShhNp) on Western Blots, despite normal detection of the Shh pro-protein (Casillas and Roelink, 2018). We and others (Traiffort et al., 2004) initially incorrectly interpreted this as a failure of auto-processing, but the same low levels were observed analyzing these mutants in Shh-C199*, a Shh mutant truncated at the auto-processing site (ShhN) (Roelink et al., 1995). Addition of the proteasome inhibitor MG132 (Lee and Goldberg, 1996) or the inhibitor of endosome acidification by chloroquine resulted in ShhN accumulation of Shh-C199*/H183A (ShhN/H183A), possibly indicating a misfolded protein-induced degradation of this mutant (Figure 2D). The Dynamin inhibitor Dynasore (that inhibits endocytosis) (Macia et al., 2006) causes strong accumulation of Shh-C199*, but not of Shh-C199*/H183A, further indicating that the destabilization of Shh-C199*/H183A occurs before it reaches the plasma membrane (Figure 2E). We found that other zinc coordination mutations as well as several holoprosencephaly-associated point mutations in Shh cause its destabilization, indicating a role for increased ShhN degradation in this birth defect (Casillas and Roelink, 2018). In general, we will not use these mutants with a reduced half-life.

The putative catalytic activity of Shh is required for association with the ECM

M15A metallopeptidases contain a zinc in their catalytic cleft that is required for catalysis as it enables the nucleophilic attack on the substrate. To further assess if ShhN is a peptidase, we asked if the accumulation of Shh-C199* in the ECM requires zinc, thus supporting the hypothesis that Shh is a zinc-peptidase. The K_d for zinc binding to Shh in the absence of calcium appears to be very low (Day et al., 1999), but the EC_{50} of Thermolysin (a well-studied calcium-regulated zinc peptidase) for zinc is about 2 µM (Holmquist and Vallee, 1974). This leaves open the possibility that the putative Shh-associated peptidase activity also requires low µM zinc concentrations to function. DMEM tissue culture medium has no added zinc and is thus expected to have only small amounts of this ion. While the amount of protein in the lysate of HEK293T cells transfected with *Shh-C199** remained relatively unchanged with increasing zinc concentrations, the amount of ECM-bound Shh-C199* increased several-fold with an EC_{50} between 0.1 and 1 µM zinc (Figure 3 B-F). This effect on ShhN ECM accumulation was specific to zinc as other divalent cations like copper and magnesium failed to increase the amount of ShhN in the ECM (Figure 3 supplemental figure 1).

Besides the zinc coordinating residues, the glutamic acid residue at position 177 (mouse Shh numbering) is predicted to be required for the first step of catalysis by providing a reactive hydroxide. The mutants Shh-C199*/E177A and -/E177V are therefore predicted to be catalytically inactive (Fuse et al., 1999). Unlike the zinc coordination mutants, we found the Shh-C199*/E177A and -/E177V mutants to be more stable and used the Shh-C199*/E177V as a mutant predicted to lack catalytic activity. Shh-C199*/E177V

failed to further accumulate in the ECM under increasing zinc concentrations, indicating that the putative zinc-peptidase activity of Shh is required for ECM association (Figure 3 B), and that the zinc effects are not primarily mediated by another zinc-peptidase or zinc sensitive event. As E177 is not required for zinc binding, a purely stabilizing effect of zinc on ECM-associated Shh can be excluded. The accumulation of Shh in the ECM is correlated with the non-cell autonomous signaling efficacy. Co-culturing LightII cells (Taipale et al., 2002) with transfected fibroblasts allows us to strictly measure non-cell autonomous signaling, and we found that in the presence of increasing concentrations of zinc, non-cell autonomous signaling is enhanced. This effect of zinc was not observed in co-cultures with *Shh-C199*/E177V*-transfected fibroblasts, further indicating that zinc affects an intrinsic property of Shh that enhances non-cell autonomous signaling (Figure 3E). This zinc effect was much less obvious when calcium concentration was increased to 1.8 mM, an effect that we address in Figure 4.

Mutating other residues predicted to stabilize Shh-substrate intermediates affect its association with the ECM

Zinc peptidase-mediated proteolysis starts by the generation of a hydroxide from water by binding of a proton to the conserved E177 equivalent. The zinc-stabilized hydroxide attacks the substrate peptide bonds via a transition state that in turn is stabilized by H135 and H181. These two histidine residues are conserved between Shh and BacHhs, but either one can be a tyrosine residue in M15A peptidases, and a tyrosine residue is present in the position homologous to H181 in butterfly and moth Hhs (e.g. NCBI PCG69308.1). We mutated either or both histidine residues 135/181 into alanine or tyrosine residues (*Shh-C199*/H135Y*or*A*, *Shh-C199*/H181Y*or*A*) and found that these forms of Shh process normally and are stable (data not shown). Mutants with one or two tyrosine substitutions as well as single alanine substitutions were found at lower levels in the ECM but could be rescued under high zinc conditions (1, 10 µM), suggesting that tyrosine residues can facilitate the coordination of the substrate intermediate. Only *Shh-C199*/H135A/H181A*, which is predicted to be unable to stabilize the transition state intermediate and consequently mediate catalysis, poorly associated with the ECM in the presence of zinc. As H135 and H181 could affect zinc binding to the catalytic site of Shh, we tested if these mutants had an altered EC_{50} for zinc. We found that all mutants have a similar EC_{50} (Figure 3D), consistent with the notion that these residues are not directly involved in zinc coordination and the initial stabilization of the reactive hydroxide. Together with *Shh-C199*/E177V*, our findings using *Shh-C199*/H135A/H181A* further support the notion that a ShhN-associated peptidase activity is required for ECM association.

The peptidase domain of a BacHh is unable to facilitate association with the ECM

To test if bacterial Hhs could substitute for the putative catalytic activity of Shh, we made a construct coding for a chimeric protein consisting of the N-terminal 65 residues of Shh, the calcium and zinc binding domains of *Bradyrhizobium paxllaeri* BacHh (codon optimized for expression in mammalian cells), followed by an

HA tag replacing the bacterial stop codon, followed by the last 10 residues of Shh up to G198 (Shh/BacHh^{HA}, Figure 3F diagram). As a control, we positioned an HA tag at the same distance (10 residues) from the C-terminus of Shh-C199* (Shh^{HA}-C199*). We found that Shh^{HA}-C199* behaved indistinguishable from Shh-C199* and entered into the ECM in a zinc-dependent manner. In contrast, although readily detected in the lysate and stabilized by Chloroquine, no Shh/BacHh^{HA} could be detected in the ECM (Figure 3F). This indicates that the bacterial peptidase activity is not sufficient for entry into the ECM and suggests that *Bradyrhizobium paxllaeri* BacHh lacks the specificity for the substrate or ECM binding partner that is recognized by Shh.

Shh-C199* mutants unable to bind calcium remain sensitive to zinc

The overall structure of ShhN and the BacHhs indicate that they consist of a regulatory calcium-binding and a catalytic zinc coordinating domain (Rebollido-Rios et al., 2014), making up most of ShhN outside the extreme N-terminal Ptch1-binding domain. With the exception of BacHhs, bacterial M15A metallopeptidases lack the Hh/BacHh-type calcium coordination domain, and this domain is thus unlikely to be required for catalytic function *per se*. We made a Shh-C199* mutant that lacked all calcium-coordinating residues (Shh-C199*/E90A/E91D/D96A/E127A/D130N/D132L, Shh-C199*-Ca^{Free}) and this form of Shh should be unable to bind calcium. After transfection, more ShhN was detected in lysates of cells cultured in the presence of higher calcium levels, but that was also observed in the Shh-C199*-Ca^{Free} expressing cells, and thus unlikely a direct effect of calcium on Shh. Increased amounts of ShhN in the lysate at higher calcium concentrations complicated the interpretation of the effects of calcium on ShhN accumulation in the ECM. However, while ShhN accumulation in the ECM varied with calcium concentrations, that of the Shh-C199*-Ca^{Free} mutant remained at the same level, indicating that this mutant is insensitive to extracellular calcium as measured by ECM association.

One possible mechanism of calcium regulating peptidase activity would be by affecting zinc coordination, thereby changing its K_d for zinc. We therefore tested if the EC_{50} of zinc is different under high (1.8 mM, the concentration in regular DMEM) and low (0.18 mM, the lowest concentration the cultured cells appeared normal) calcium. Under low calcium conditions, the addition of 5 μM zinc to the medium resulted in increased accumulation of ShhN in the ECM both of Shh-C199*-Ca^{Free} and Shh-C199* (Figure 4B). This indicates that Shh-C199*-Ca^{Free} is still able to mediate the putative catalytic event for ECM accumulation, and supports the notion that calcium binding is not required for Shh-mediated catalysis. E127 is located at the interface between the calcium and zinc-binding domains of Shh, and we tested if restauration of this residue in Shh-C199*-Ca^{Free} affects ECM localization but found little or no difference (Figure 4B). To better quantify the effect of calcium and zinc on Shh-C199* and Shh-C199*-Ca^{Free} in their ability to accumulate in the ECM we used ELISA directly on the de-cellularized ECM. Under low calcium conditions we found that the response to increasing zinc concentrations was similar between Shh-C199* and Shh-C199*-Ca^{Free}.

For both, the EC_{50} for zinc appeared to be around 0.1 µM. Instantiated in Figure 4B and quantified over multiple experiments in Figure 4C, it appears that Shh-C199*-Ca^{Free} is less efficient in entering the ECM than Shh-C199*. This effect was more profound in the presence of 1.8 mM calcium, and much more Shh-C199* was detected in the ECM than Shh-C199*-Ca^{Free} in the absence of added zinc. The addition of zinc had a bigger effect on Shh-C199*-Ca^{Free} than on Shh-C199*. These results indicate that Shh-C199*-Ca^{Free} behaves similarly in high and low calcium and resembles Shh-C199* under low calcium. Thus, whereas the behavior of Shh-C199* changes as a function of calcium, that of Shh-C199*-Ca^{Free} does not, indicating that binding of calcium to Shh alters its intrinsic properties as measured by its association with the ECM.

Distribution of cholesterol-modified ShhNp in the ECM differs from cholesterol-unmodified ShhN but is zinc sensitive

While ShhN could readily be detected in the ECM of HEK293T cells, processed ShhNp poorly accumulated in the ECM, possibly reflecting earlier bottlenecks, like processing (Lee et al., 1994), Dispatched1 activity (Ma et al., 2002) and re-internalization. As ShhN can be internalized via several Shh-binding proteins, (Incardona et al., 2000; McCarthy et al., 2002; Wilson and Chuang, 2010) we assessed if expression of Shh in cells lacking many of its binding partners altered ECM accumulation. Staining for Shh in the ECM of transfected fibroblasts lacking many Shh (co)-receptors (*Ptch1*$^{LacZ/LacZ}$;*Ptch2*$^{-/-}$;*Boc*$^{-/-}$;*Cdo*$^{-/-}$;*Gas1*$^{-/-}$) showed that ShhN was present in small puncta that gave a cloudy appearance at lower magnifications. 5 µM zinc increased the number of these small puncta, which could be quantified by measuring the fluorescence intensity across the entire image area (Figure 5 B). In contrast, cholesterol-modified ShhNp was detected in larger puncta in a more restricted area. While the distribution of large ShhNp puncta with increasing zinc was largely unaffected, we detected an increase in small puncta with a wider distribution resembling ShhN distribution. The effects of zinc on Shh distribution in the presence of 1.8 mM calcium was much less pronounced, further supporting the finding that high calcium negatively affects the zinc-dependent activity of Shh.

To assess if the observed effects require the putative peptidase activity of Shh we tested ShhE177A, and -H181Y. Consistent with the biochemical observations using Shh-C199* (Figures 2, 3), we could barely visualize ShhE177A in the ECM. In contrast, ShhH181Y distribution into the ECM was indistinguishable from Shh, further indicating that this “butterfly version” of Shh is active. Together, our results provide evidence that an intrinsic property of Shh, likely a peptidase activity, is activated by zinc and regulated by calcium mediates its association with the ECM.

Discussion

Here, we provide evidence for a function of Shh as a peptidase that is required for the association of Shh to the ECM. Zinc is a potent agonist of this putative peptidase activity as it increases ECM association of

Shh but not of putative peptidase mutants. The observations that Shh-E177A is unable to mediate signaling from the notochord to the overlying neural tube (non-cell autonomously), and is more capable than Shh to induce the Hh response when expressed in the developing neural tube (likely cell-autonomously) (Himmelstein et al., 2017), provides in vivo evidence that the putative zinc-peptidase activity of Shh is required for non-cell autonomous signaling, but not for the activation of the Hh response *pe se*. The initial experiments that demonstrated that E177 is dispensable for the activation of the Hh response is easily explained as this mutant ligand was added to the responding cells as a purified and soluble fraction (Fuse et al., 1999), thus bypassing the requirement for the peptidase function that we propose. Our observations that the catalytic domain of ShhN is required for its localization to the ECM provides further evidence that Shh is a peptidase, and that this activity is required for non-cell autonomous signaling. Distinct from the peptidase domain is the extreme N-terminal end of ShhN which binds to Ptch1 (Gong et al., 2018; Qi et al., 2018a; 2018b) and suffices to alter Ptch1 activity (Tukachinsky et al., 2016), further demonstrating the dispensability of the peptidase activity to activate the Shh response.

Do Bacterial Hhs and Shh share a peptidase activity?

Our observations indicate that Shh distribution away from the sites of synthesis and non-cell autonomous Shh signaling can be enhanced under low-calcium and high zinc conditions. The surprising sequence similarity between bacterial and mammalian Hedgehog proteins strongly suggest they have similar functions. The organization of bacterial genomes into operons helps in the assignment of possible functions of unknown proteins. The suggested role of BacHh (as a M15A peptidase (Rawlings and Barrett, 2013)) in the modification of the bacterial peptidoglycans is further supported by the observation that in *Mesorhizobium* and *Bradyrhizobium* the *BacHh* gene is surrounded by genes (likely constituting an operon) that code for proteases, including lysozyme, N-acetylmuramoyl-L-alanine amidase, a peptidoglycan endopeptidase (peptidase M23A), several Trypsin homologs (peptidase S1), a zinc Matrix Metalloprotease (MMP) homolog (peptidase M54), an endonuclease, peptidase S53, and possibly a Phytase (DUF3616). This complex of enzymes might be involved in bacterial feeding or scavenging. BacHhs in *Rhizobiacea* are not part of the core genome (González et al., 2019), as the majority of these bacteria do not carry *BacHh*, a further indication that BacHhs provide a niche-specific specialized function.

M15 peptidases cleave peptidoglycans, the major component of the bacterial periplasmic space, and a major component of detritus. Peptidoglycans are analogs of proteoglycans that are common in extracellular matrix (ECM) of animals. Therefore, it is possible that functional conservation between BacHhs and Shh is reflected in the ability of Shh to cleave or modify proteoglycans, thus affecting the Shh response and/or distribution, independent of its binding to the canonical Hh receptors. Although any Shh antagonist could be a possible target for Shh peptidase activity, the Hh-interacting protein (Hhip) is an unlikely candidate as it binds to Shh via the zinc ion, thereby replacing the catalytic water. This mode of binding is akin to that of

a metalloprotease/inhibitor interaction (Bosanac et al., 2009), and thus likely to inhibit the putative catalytic function of Shh instead of being a substrate. The targets for penicillin and related antibiotics are peptidoglycan peptidases, leaving open the development of nM drugs that inactivate the peptidase activity of Shh, and thus be powerful inhibitors of non-autonomous Shh signaling that underlies several cancers.

Are Hhs proteoglycan peptidases?

Hedglings and Hedglets are related to Hhs, and the conserved domains possibly homologous. All animals that have Hedglet also have a *Hh* gene and it is thus plausible that Hedglets are derived from Hh. Hhs are not found in any eukaryote except *cnidarians* and bilaterians. The distribution of Hedgling and Hhs only overlaps in *cnidarians*, but Hedgling can also be found in sponges and choanoflagellates (Figure 1, supplemental Figure 1). This suggests two evolutionary events giving rise to these proteins; one occurring in a *Choanoflagellate* ancestor that originated the gene coding for Hedgling, and an independent event in a *Cnidarian* ancestor that gave rise to modern Hh. The absence of both Hedgling and Hh from algae, plants, fungi, in addition to almost all unicellular eukaryotes makes it unlikely that both Hh and Hedgling linearly evolved from a BacHh protein that could have been present in the Ur-eukaryote, but more likely are products of more recent gene transfers from bacteria. The distribution among eukaryotes of Glypicans and Hs is overlapping, and both are first observed in *Cnidarians* and present in all bilaterians. A more recent evolutionary relationship between BacHh and Hhs is further supported by the observation that the C-terminal residue of many BacHhs perfectly aligns with the exon 2 splice donor site in *Hh* genes, thereby providing a parsimonious explanation how a *BacHh* gene was incorporated in a eukaryotic genome giving rise to *Hh*. This is in contrast to the much less conserved Hh domain in Hedgling that is encoded within a single large exon. Given the central role of Gpcs in the distribution of and response to Hhs (including Shh), Glypicans and Hhs might have co-evolved possibly as a peptidase/substrate combination, co-opting the peptidoglycan activity of BacHhs to cleave the proteoglycan Glypican. Hh-like bacterial peptidases (M15A) are predicted to be carboxy(trans)peptidases, cleaving adjacent to the D-ala that is linked to the murein glycans (Bochtler et al., 2004; Vollmer and Bertsche, 2008). By analogy, Shh might cleave an unusually modified C-terminal residue. It is intriguing that the C-termini of Glypicans are linked to the GPI anchor that restricts them to the cell surface (Filmus et al., 1995). Solubilization of Shh-sequestering Gpcs by GPI removal would elegantly reconcile the observed peptidase-dependent entry of Shh into the ECM with the important effects of Gpcs on Shh signaling and distribution.

It is perhaps unfortunate that Hh was discovered in *Drosophila,* as of all animals sequenced, only Hh in *Drosophilids* is divergent for two of the three residues that coordinate zinc and lacks the critical E177 equivalent. The predicted lack of peptidase activity in *Drosophilid* Hhs is remarkable and further supports the observation that the putative peptidase activity is not required for the Hh/receptor interaction. Perhaps stricter reliance on cytonemes in *Drosophila* that detect Hh at its source (Huang et al., 2019) renders the

ancestral peptidase activity obsolete. Nevertheless, this loss of the putative peptidase activity is unique to *Drosophilids*, as all other (sequenced) animals retain the typical zinc coordination motif and the associated E177 equivalent that are required for catalytic activity. Based on the loss-of-function of several mutants, this intrinsic property is likely a zinc metallopeptidase activity, just like the bacterial counterparts of Shh. Still, the observation that substitution of the Shh calcium/zinc domains with those of BacHh results in a protein that does not enter the ECM, indicates that their substrates are not interchangeable.

Although mutations of the central zinc coordinating triad are unstable and thus cannot be easily assessed for loss of peptidase function, mutations of several other catalytically important residues (E177, H135 and H181) are not destabilized and show a loss in the ability of Shh to enter the ECM. Together with the observation by Himmelstein and colleagues (Himmelstein et al., 2017) that ShhE177A cannot signal from the notochord to the overlying neural plate strongly supports the idea that a Shh-associated peptidase activity is required for non-cell autonomous signaling by promoting its distribution away from the source cells.

Material and Methods

Sequence analysis

Bacterial Hedgehogs, Hedglings and Hedglets were identified via protein-protein BLAST (NCBI) and HMMER (ensemble) searches (Gish and States, 1993) using the peptide sequence of the Shh N-terminal domain as the initial query sequence. Conserved sequences were manually curated to contain only the calcium and zinc coordination domains (around 105 residues). Sequences (supplemental file) were aligned in Clustal Omega (EMBL-EBI). An average distance tree and a PCA plot were generated in Jalview (Waterhouse et al., 2009), using the BLOSUM62 algorithm. Visualizations of the ShhN structure were generated in UCSF Chimera using Protein Database (PDB) ID 3D1M (McLellan et al., 2008).

Materials

MG-132 and Concanamycin A were from Calbiochem, Chloroquine and $ZnCl_2$ from Sigma, $CaCl_2$ from Fisher Scientific, and Dynasore from Abcam.

Cell culture

Ptch1$^{-/-}$*;Ptch2*$^{-/-}$ fibroblasts were derived from mouse embryonic stem cells and are described elsewhere (Casillas and Roelink, 2018) . All cells were cultured in DMEM (Invitrogen) supplemented with 10% FBS (Atlas Biologicals). Cells were transfected using Lipofectamine2000 reagent (Invitrogen) according to the manufacturer's protocol.

DNA constructs

The following mutations were created via site-directed mutagenesis: *Shh-C199*/E177V, Shh-C199*/H135A, Shh-C199*/H135Y, Shh-C199*/H181A, Shh-C199*/H181Y, Shh-C199*/H135A/H181A, Shh-C199*/H135Y/H181Y, Shh-C199*/E90A/E91D/D96A/D130N/D132L, Shh-C199*/E90A/E91D/D96A/E127A/D130N/D132L*. *Bradyrhizobium paxllaeri BacHh* (EnsemblBacteria: LMTR21_38280, NCBI: WP_065756078.1) was codon optimized for eukaryotic expression using the IDT DNA Codon Optimization Tool, ordered as a gBlocks gene fragment from IDT DNA, and cloned into pcDNA3.1(+). Both the *Shh-C199** vector backbone including the Shh N- and C-terminus as well as the calcium and zinc coordination domain of *Bradyrhizobium paxllaeri BacHh* were PCR amplified, separated on a 1% agarose gel, and extracted with MinElute columns (QIAGEN). The fragments were cut with *BsaI* and ligated with T4 DNA ligase according to the Golden Gate cloning protocol (New England Biolabs).

Immunostaining

Ptch1$^{-/-}$*;Ptch2*$^{-/-}$ fibroblasts were plated on 12mm glass cover slips and transfected with *Shh-C199** the following day and subsequently allowed to recover for 24h. The transfected cells were then incubated for

24h in serum-free DMEM containing varying concentrations of $CaCl_2$ or $ZnCl_2$, the cells were detached from the cover slip with PBS. The cover slips were washed with PBS at least 5 times and blocked with 10% heat-inactivated goat serum in PBS with 0.1% TritonX (PBS-T). Mouse α-Shh (5E1, Developmental Studies Hybridoma Bank) was used at 1:30 in blocking solution and goat α-mouse Alexa568 secondary antibody (Invitrogen) at 1:1,000 in blocking solution. Shh distribution was visualized with a Zeiss Observer at 10x and 63x magnification.

Western Blot/SYPRO ruby staining

HEK293T cells were plated in 12 well plates and transfected with Shh mutants as indicated the next day. 24h after transfection, the medium was switched to serum free DMEM with the indicated calcium and zinc concentrations overnight. Cells were then detached from the plate with PBS and lysed in a microcentrifuge tube with RIPA buffer (150 mM NaCl, 50 mM Tris-HCl, 1% Igepal, 0.5% Sodium Deoxycholate, and protease inhibitors). The lysate was incubated for 30 min on ice and cleared by centrifugation. For isolation of ECM-bound Shh, the decellularized tissue culture dish was washed with PBS and deionized water at least 5 times and scraped with a cell scraper and 5X SDS sample buffer heated to 95°C, as described (Hellewell et al., 2017). A fifth of the sample was run on a 12% SDS-PAGE gel and transferred to a 0.45μ nitrocellulose membrane. Membranes were blocked in 5% milk in Tris-buffered saline with 0.1% Tween-20 (TBS-T) and incubated with a polyclonal rabbit α-Shh antibody (H2, 1:10,000) (Roelink et al., 1995) in blocking solution, followed by incubation with a goat α-rabbit Alexa647 secondary antibody (Invitrogen, 1:10,000) in blocking solution. GAPDH was used as a loading control (Rabbit α-GAPDH, 14C10, Cell Signaling Technologies). Western Blots were visualized with a ChemiDoc visualization system (Bio-Rad).

Alternatively, the SDS-PAGE gel was stained with SYPRO-Ruby gel stain (Thermo-Fisher) according to the manufacturer's instructions and visualized with a ChemiDoc visualization system (BioRad).

ELISA

HEK293T cells were plated in 96 well plates and transfected with *Shh-C199** and *Shh-C199*/E90A/E91D/D96A/E127A/D130N/D132L* in triplicates the next day. 24 h after transfection, the medium was replaced with DMEM containing 0.18 mM or 1.8 mM Calcium and Zinc concentrations ranging from 0.001 to 1 μM for 48 h. The cells were removed from the plate with PBS and deionized water. The plates were blocked with PBS + 5% heat-inactivated goat serum, incubated with mAB5E1, followed by an HRP conjugated α-mouse secondary antibody (Invitrogen). Western-Lightning Plus-ECL (Perkin Elmer) was added to the wells and luminescence was measured in a Wallac Victor3 plate reader (Perkin Elmer).

Non-cell autonomous signaling assay

Ptch1$^{-/-}$;*Ptch2*$^{-/-}$ fibroblasts were plated in 24 well plates and transfected with the indicated *Shh-C199** variants the next day. 24h after transfection, cells were washed with PBS once and LightII reporter cells (Taipale et al., 2000) were added. As soon as cells were adherent, the medium was switched to DMEM containing the indicated zinc and calcium concentrations. 48h later, the cells were lysed and luciferase activity was measured using the Dual Luciferase Reporter Assay System (Promega). Firefly luciferase measurements were normalized against Renilla luciferase measurements for each technical replicate to control for differences in cell growth. Firefly/Renilla luciferase values were then normalized to the mock control average for each experiment.

Genome editing: *Ptch1*$^{LacZ/LacZ}$;*Ptch2*$^{-/-}$;*Boc*$^{-/-}$;*Cdo*$^{-/-}$;*Gas1*$^{-/-}$;*Shh*$^{-/-}$ were derived from *Ptch1*$^{LacZ/LacZ}$;*Ptch2*$^{-/-}$;*Shh*$^{-/-}$ cells (Roberts et al., 2016). TALEN constructs targeting the first exon of mouse *Cdo* and *Gas1* were designed and cloned into the pCTIG expression vectors containing IRES puromycin and IRES hygromycin selectable markers (Cermak et al., 2011). The following repeat variable domain sequences were generated: Cdo, 5' TALEN: NN HD NI NG HD HD NI NN NI HD HD NG HD NN NN ; 3' TALEN: HD NI HD NI NI NN NI NI HD NI NG NI HD NI NN; Gas1, 5' TALEN: NN NI NN NN NI HD NN HD HD HD NI NG NN HD HD; 3' TALEN: NN NN NI NI NI NI NN NG NG NG NN NG HD HD NN NI. Two CRISPR constructs targeting a double strand break flanking the first exon of mouse Boc were cloned into pSpCas9 vector with an IRES puromycin selectable marker (Ran et al., 2013). The Boc CRISPRs targeted the following forward genomic sequences (PAM sequences underlined): Upstream of first exon 5' CCTGTCCTCGCTGTTGGTCCCTA 3'; Downstream of first exon 5' CCCACAGACTCGCTGAAGAGCTC 3'. *Ptch1*$^{LacZ/LacZ}$;*Ptch2*$^{-/-}$;*Shh*$^{-/-}$ mouse embryonic stem cells (Roberts et al., 2016) were transfected with 6 genome editing plasmid. One day after transfection, ES medium with 100 ug/mL hygromycin and 0.5 ug/mL puromycin was added for 4 days. Surviving mESC colonies were isolated, expanded and genotyped by sequence PCR products spanning TALEN and CRISPR-binding sites. PCR screening was performed on cell lysates using primers flanking the TALEN or CRISPR binding sites for the *Boc*, *Cdo*, and *Gas1* loci. *Boc*, (5') CATCTAACAGCGTTGTCCAACAATG and (3') CAAGGTGGTATTGTCCGGATC; *Cdo*, (5') CACTTCAGTGTGATCTCCAG and (3') CCTTGAACTCACAGAGATTCG; Gas1, (5') ATGCCAGAGCTGCGAAGTGCTA and (3') AGCGCCTGCCAGCAGATGAG. PCR products were sequenced to confirm allele sequences. A *Ptch1*$^{LacZ/LacZ}$;*Ptch2*$^{-/-}$;*Boc*$^{-/-}$;*Cdo*$^{-/-}$;*Gas1*$^{-/-}$;*Shh*$^{-/-}$ mESC clone was identified harboring a 50 bp deletion in Cdo exon 1, a heteroallelic 480 bp insertion and a 200 bp deletion in Gas1 exon1 resulting in a premature stop codon in the reading frame, and a 450 bp deletion of Boc exon 1. These cells were transfected with *LargeT* and *myc*, and deprived of Lif to generate immortalized fibroblasts.

Data Analysis: Single Factor ANOVA was used to analyze more than two conditions, followed by a Student's *t*-test with a two-tailed distribution assuming unequal variance comparing two conditions. **p*<0.05, ***p*<0.01, ****p*<0.001, *****p*<0.0001.

Acknowledgements.

This work was supported by NIH grant 1R01GM117090 to HR. We thank Drs. N. King and D. Rokhsar for discussions on Hh evolution, and Dr. C. Casillas for help with the receptorless cell line. All experiments were performed by CJ. Experiments were designed by CJ and HR. The manuscript was written by CJ and HR.

The authors declare no conflict of interest.

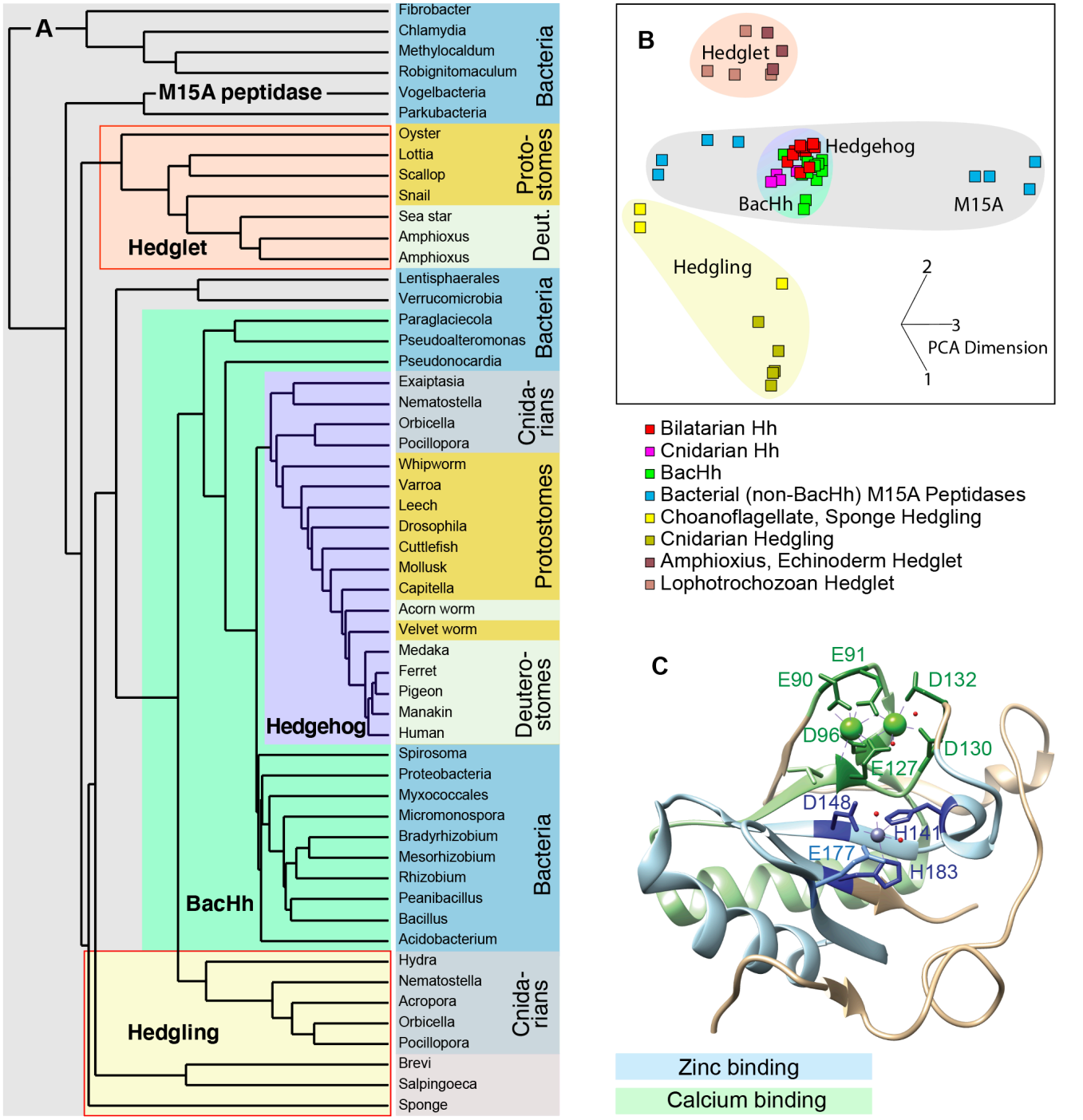

D

```
DIVFKDEEGTGADKVMSKRMKEKLDKLAELVKKEWPSLKLRVTECWDENNEHSSNSTHYEGRGADLTTSDVDKSKLGRLGQLAVDAGLDWVFYENDAHIHVSVKK BacHh
DIIFKDEENTGADRLMTQRCKDKLNALAISVMNQWPGVKLRVTEGWDEDGHHSEESLHYEGRAVDITTSDRDRSKYGMLGQLAVDAGLDWVFYENDAHIHVSVKK Hh
NTNSEIVFANDDCRRMTARAKSKLDVLGSRVKRQWSNAKLKVLLAWDQIIPQAPISLHYEGRALRLQTSDGDRKKLSTLAGLAVQAGFDWVHYATSSYIHASVIR Hedgling
```

Figure 1: ShhN-related sequences are present in animals and bacteria.

A: A similarity tree of Hh sequences encompassing the calcium and zinc coordinating domains. All Hhs are closely related and root from within the BacHhs. Hedglings (present in Choanoflagellates, Sponges, and Cnidarians) and Hedglets (present in Lophotrochozoans, Amphioxus and Echinoderms) form outgroups, but all are related to bacterial M15 peptidases. Organisms in the same phylum or clade are

color coded, and common names of the organisms are used. Sequences and accession numbers can be found as a supplemental file. Hedglings and Hedglets (red borders) are predicted to be unable to mediate catalysis. **B:** PCA plot of the tree presented in A. **C:** Structure of Shh (3D1M) with salient residues and domains indicated. **D:** Sequence lineup of Mesorhizobium BacHh, human Dhh, and Choanoflagellate Hedgling. Identical residues are indicated in amber. Salient residues are color coded and color coordinated with C.

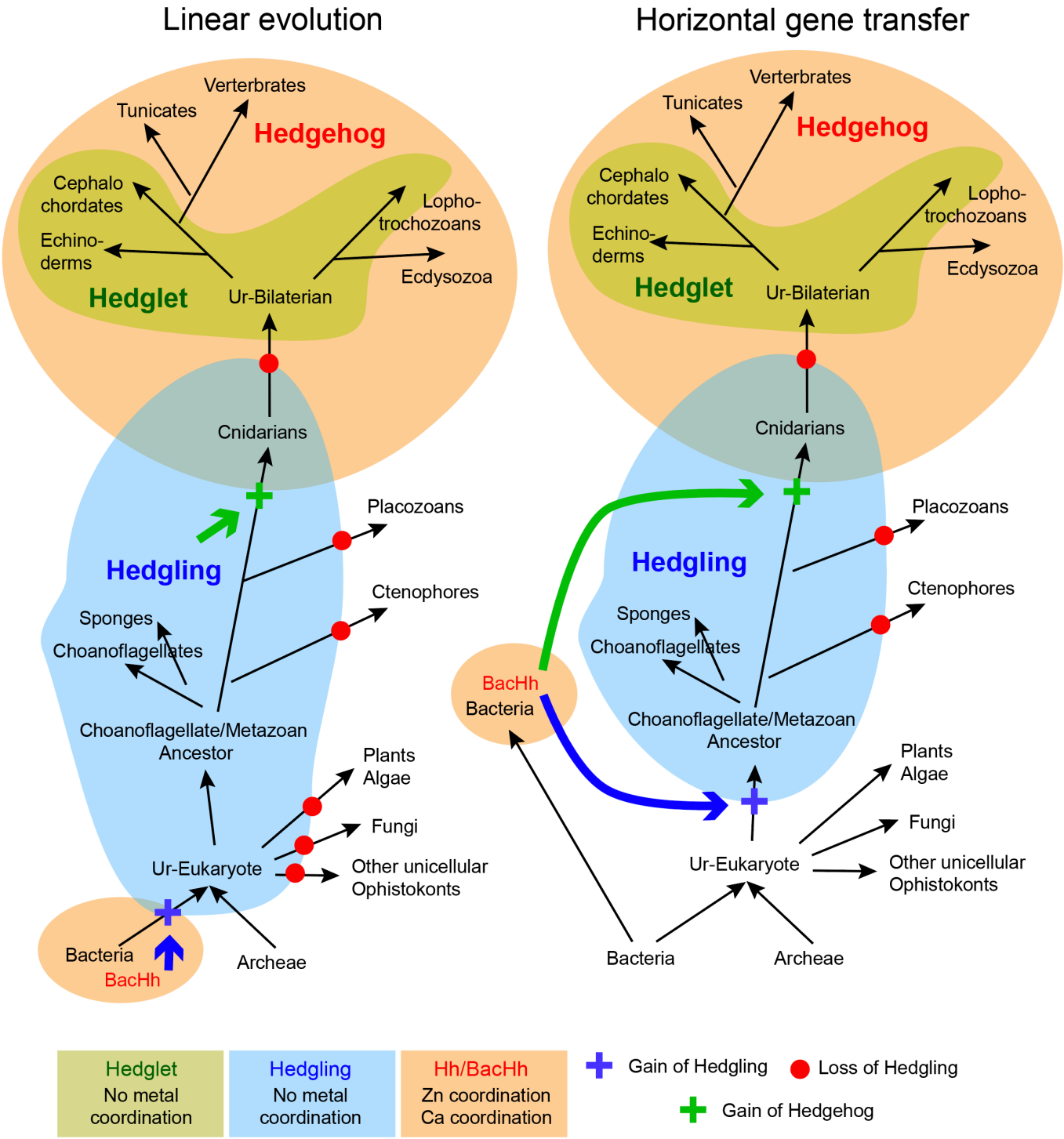

Figure 1 Supplemental Figure 1. Models for the evolution of Hh, Hedgling, and Hedglet. Although eukaryotic Hhs and their homologs could be explained by the persistence of BacHh in the Ur-eukaryote, a more parsimonious explanation involves more recent gene transfer of BacHh genes into eukaryotes

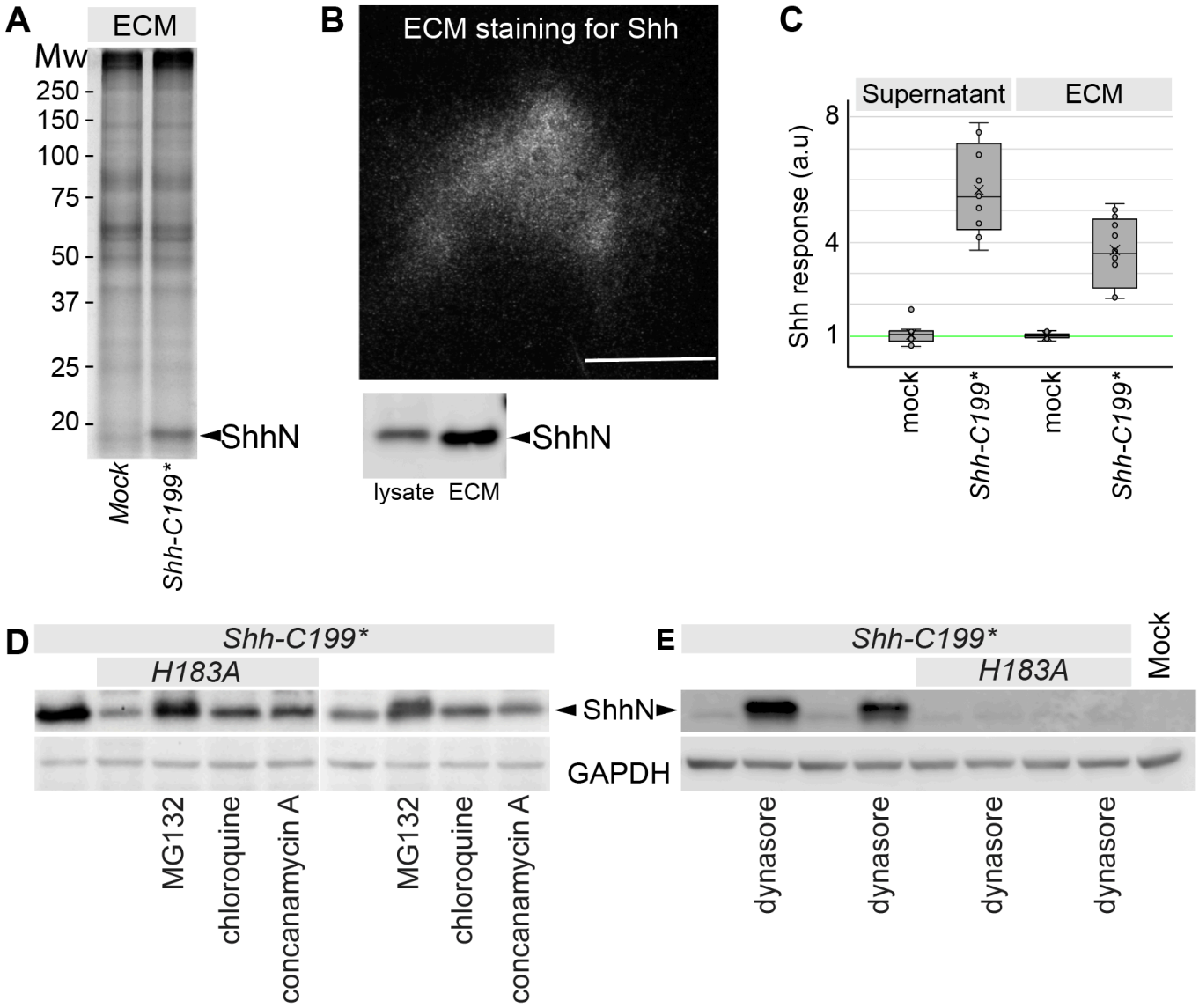

Figure 2: Active ShhN associates with the extracellular matrix.

A: ECM deposited by mock and *Shh-C199**-transfected HEK293T cells analyzed by SDS-PAGE and SYPRO-Ruby staining. ShhN is indicated. **B:** *Shh-C199**-transfected HEK293T cells were plated on glass slides and removed after 24h. The slides were stained with mAb5E1, showing the presence of ShhN. Scale bar is 50µm. **C:** supernatant and ECM conditioned by *Shh-C199**-transfected HEK293T cells. LightII cells were either grown on mock or ShhN conditioned ECM. Cells grown on ECM deposited by mock transfected cell were grown in the absence or presence of mock or Shh-C199* conditioned supernatant. Box and whisker plots, n ≤ 3. **D:** Western blot analysis of HEK293T cells transfected with the indicated Shh mutants. 100 nM MG-132 (proteasome inhibitor), 100 nM Chloroquine and 100 nM Concanamycin A (inhibitors of endosome acidification) were assessed for their ability to affect Shh accumulation. **E:** Western blot analysis of HEK293T cells transfected with the indicated Shh mutants, and the effects of the dynamin inhibitor Dynasore (50 µM) was assessed for its effect on Shh accumulation.

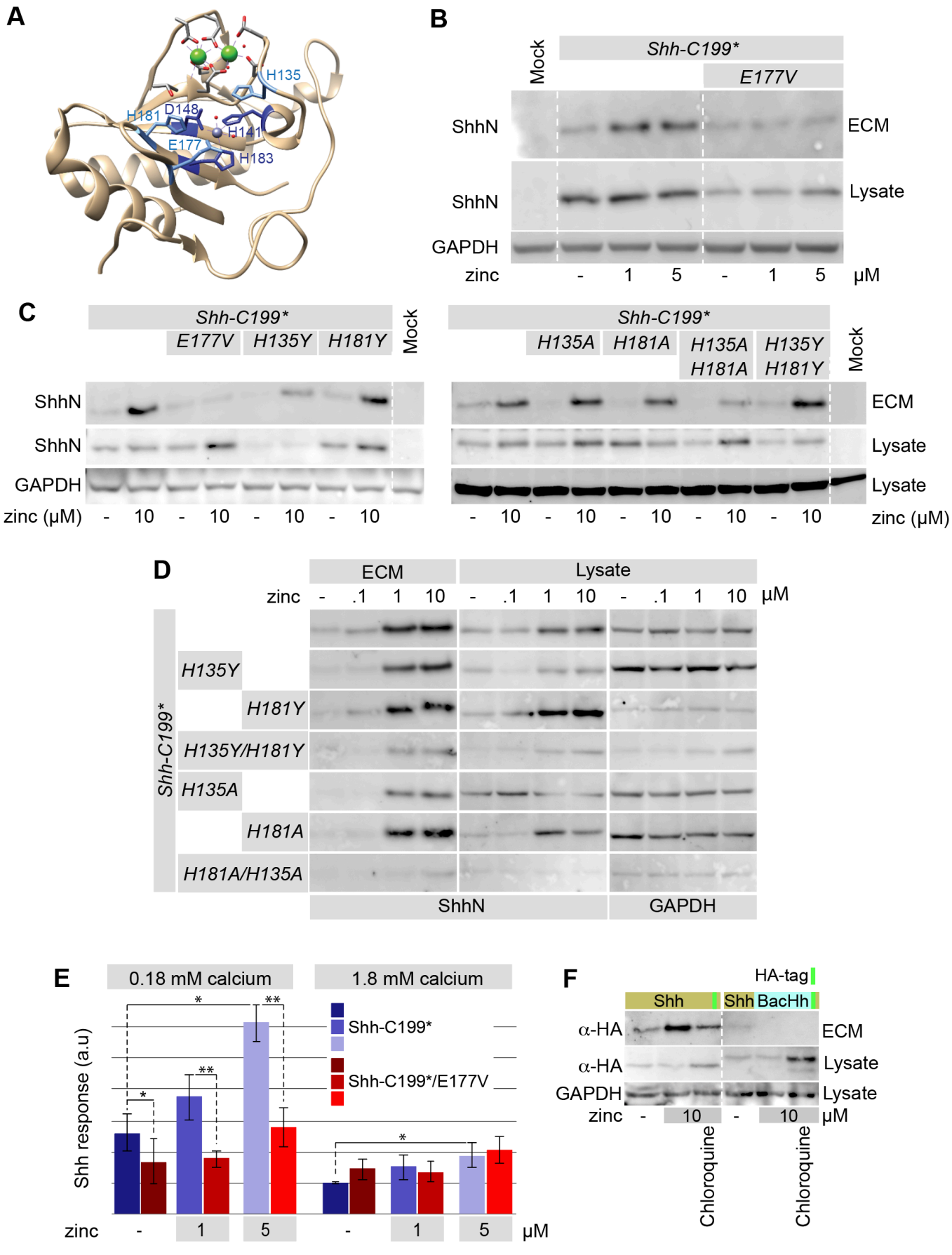

Figure 3: ECM-association of ShhN requires zinc in and putative peptidase activity. **A:** Diagram of the Shh structure (3D1M) with relevant residues indicated. **B:** Western blot analysis of the lysate and ECM of HEK293T cells transfected with *Shh-C199** and *Shh-C199*/E177V* and cultured in DMEM containing 0.18 mM calcium and the indicated concentrations of zinc. **C:** The effect of mutations of the transition state-stabilizing residues H135 and H181 to alanine (A) or tyrosine (Y) on the zinc-dependent accumulation in the ECM was analyzed on a Western Blot of the extracted ECM from transfected HEK293T cells cultured in 0.18 mM calcium with or without 10 µM zinc. **D:** zinc dose-response analysis of H135 and H181 mutations assessed by Western blot of the lysate and ECM of HEK293T cells transfected with the indicated mutants and cultured in 0.18 mM calcium and increasing concentrations of zinc (0.1, 1, 10 µM). **E:** LightII cells co-cultured with *Shh-C199** and *Shh-C199*/E177V* transfected *Ptch1*$^{LacZ/LacZ}$;*Ptch2*$^{-/-}$ fibroblasts in the presence of 0.18 and 1.8 mM calcium and the indicated zinc concentrations. Responses were normalized to Shh-C199* with 1.8 mM calcium and no zinc. Shown are means and standard errors of 3 independent experiments. *p<0.05, **p<0.01. **F:** The ability of a Shh-BacHh chimera containing the bacterial peptidase domain to associate with the ECM was assessed by Western Blot analysis of the lysate and ECM of transfected HEK293T cells. 10 µM zinc, 100 µM chloroquine was added for 24h where indicated.

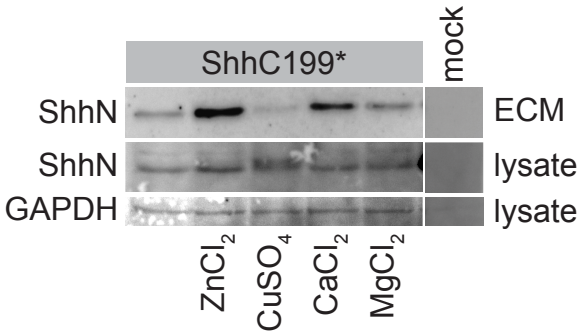

Figure3 Supplemental Figure 1: Western blot analysis of the lysate and ECM of HEK293T cells transfected with *Shh-C199** and cultured in DMEM containing 0.18 mM calcium and in the presence of 5 µM zinc, 5 µM copper, 1.8 mM magnesium or 1.8 mM calcium as indicated.

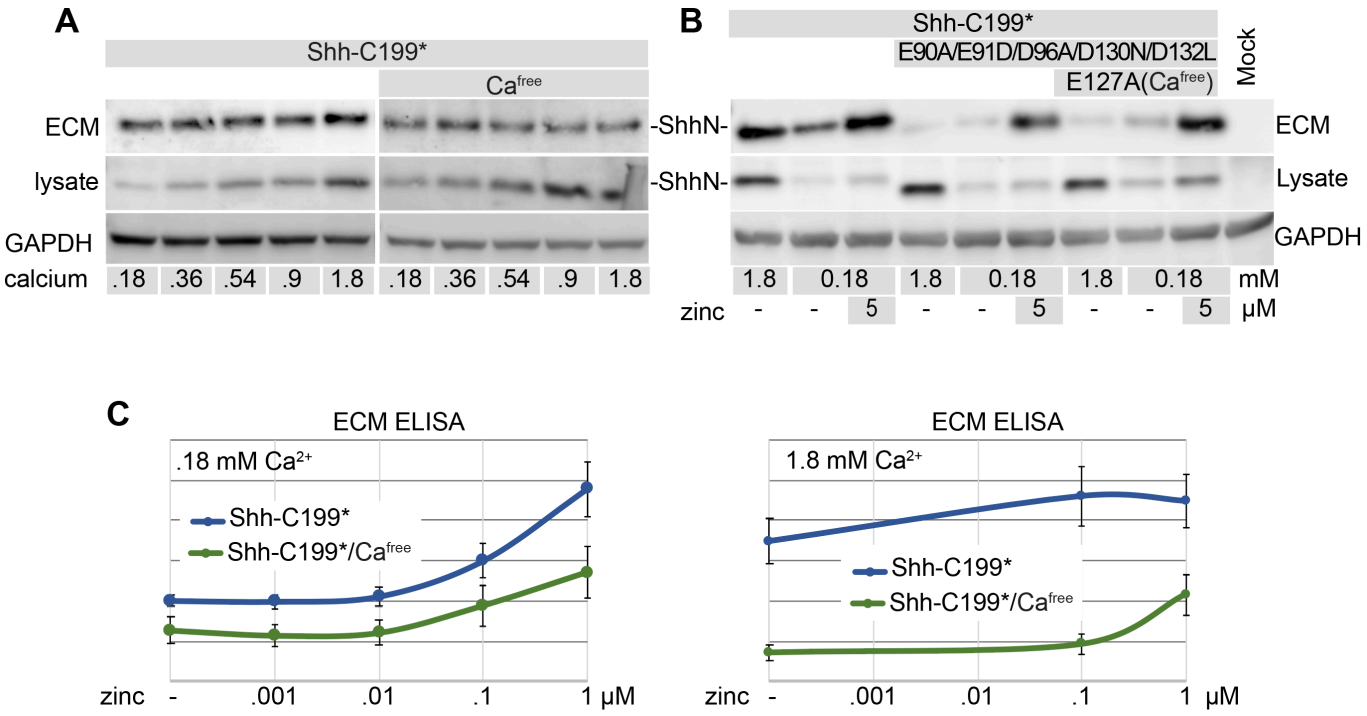

Figure 4: Calcium alters the sensitivity of Shh to zinc. **A:** HEK283T cell were transfected with *Shh-C199** and *Shh-C199*/E90A/E91D/D96A/E127A/D130N/D132L* (*Shh-C199*/Ca^{Free}*), cultured in the presence of calcium in concentrations ranging from 0.18 to 1.8 mM without added zinc, and the lysates and ECM were assessed by Western blot analysis. **B:** *Shh-C199** and *Shh-C199*/E90A/E91D/D96AD130N/D132L* , or *Shh-C199** and *Shh-C199*/E90A/E91D/D96A/E127A/D130N/D132L* (*Ca^{Free}*), cultured in the presence of 0.18 or 1.8 mM calcium, and in the absence or presence of 5 µM added zinc, and the lysates and ECM were assessed by Western blot analysis. **C:** ECM-associated Shh-C199*N or Shh-C199*/Ca^{Free} was assessed by ELISA in the presence of .18 mM calcium (left panel) or 1.8 mM calcium (right panel) and increasing zinc concentrations as indicated. Shown are means and standard errors, n=6.

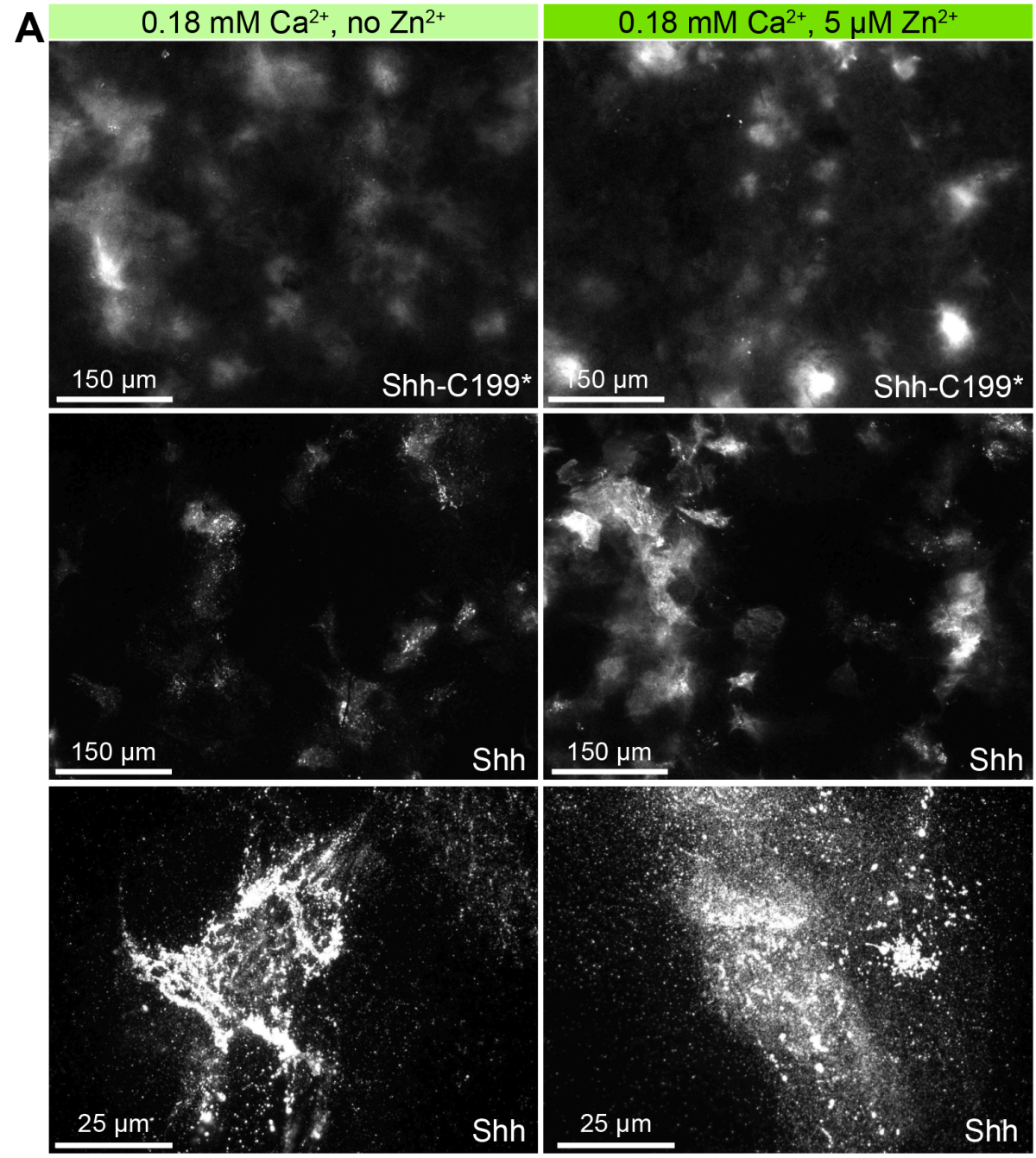

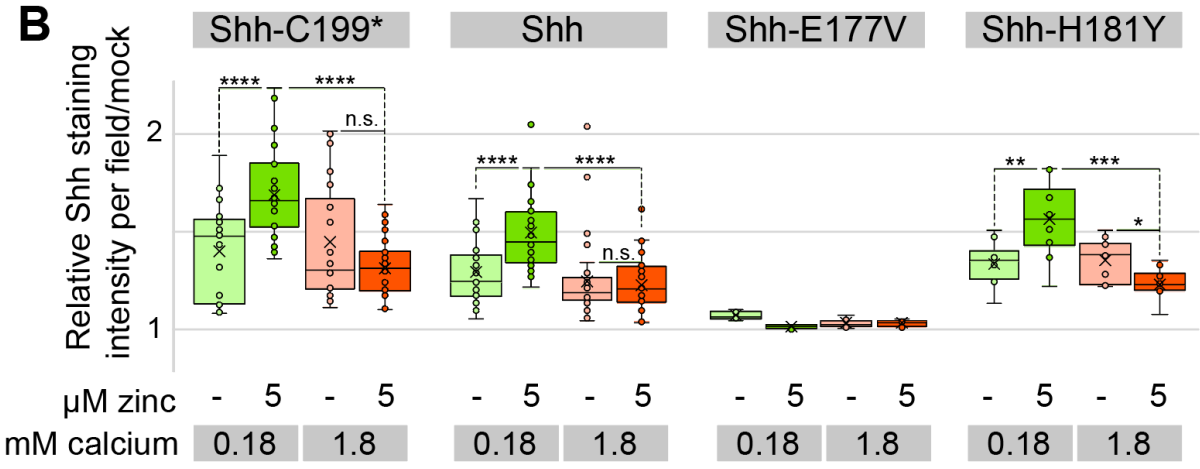

Figure 5: Cholesterol-modified ShhNp associates with the ECM in a zinc and peptidase-dependent manner. **A:** *Ptch1*$^{LacZ/LacZ}$;*Ptch2*$^{-/-}$;*Boc*$^{-/-}$;*Cdo*$^{-/-}$;*Gas1*$^{-/-}$ cells were transfected with *Shh* or *Shh-C199** and grown on glass coverslips in the presence or absence of 5 µM zinc and presence of 0.18 mM calcium. After removal of the cells the ECM was stained with mAb5E1. **B:** Box and whisker plots, quantification of ECM-bound Shh shown in A. Mean fluorescence intensity per image of 10 microscope fields without DAPI staining per experiment was measured in ImageJ and normalized to the ECM of mock transfected cells. n=3, ****p<0.0001, n.s. not significant.

References

Bellaiche, Y., The, I., and Perrimon, N. (1998). Tout-velu is a Drosophila homologue of the putative tumour suppressor EXT-1 and is needed for Hh diffusion. Nature *394*, 85–88.

Bochtler, M., Odintsov, S.G., Marcyjaniak, M., and Sabala, I. (2004). Similar active sites in lysostaphins and D-Ala-D-Ala metallopeptidases. Protein Sci. *13*, 854–861.

Bosanac, I., Maun, H.R., Scales, S.J., Wen, X., Lingel, A., Bazan, J.F., de Sauvage, F.J., Hymowitz, S.G., and Lazarus, R.A. (2009). The structure of SHH in complex with HHIP reveals a recognition role for the Shh pseudo active site in signaling. Nature Structural & Molecular Biology *16*, 691–697.

Capurro, M.I., Xu, P., Shi, W., Li, F., Jia, A., and Filmus, J. (2008). Glypican-3 inhibits Hedgehog signaling during development by competing with patched for Hedgehog binding. Developmental Cell *14*, 700–711.

Carrasco, H., Olivares, G.H., Faunes, F., Oliva, C., and Larraín, J. (2005). Heparan sulfate proteoglycans exert positive and negative effects in Shh activity. J. Cell. Biochem. *96*, 831–838.

Casillas, C., and Roelink, H. (2018). Gain-of-function Shh mutants activate Smo cell-autonomously independent of Ptch1/2 function. Mechanisms of Development *153*, 30–41.

Cermak, T., Doyle, E.L., Christian, M., Wang, L., Zhang, Y., Schmidt, C., Baller, J.A., Somia, N.V., Bogdanove, A.J., and Voytas, D.F. (2011). Efficient design and assembly of custom TALEN and other TAL effector-based constructs for DNA targeting. Nucleic Acids Res. *39*, e82.

Day, E.S., Wen, D., Garber, E.A., Hong, J., Avedissian, L.S., Rayhorn, P., Shen, W., Zeng, C., Bailey, V.R., Reilly, J.O., et al. (1999). Zinc-dependent structural stability of human Sonic hedgehog. Biochemistry *38*, 14868–14880.

Echelard, Y., Epstein, D.J., St-Jacques, B., Shen, L., Mohler, J., McMahon, J.A., and McMahon, A.P. (1993). Sonic hedgehog, a member of a family of putative signaling molecules, is implicated in the regulation of CNS polarity. Cell *75*, 1417–1430.

Fairclough, S.R., Chen, Z., Kramer, E., Zeng, Q., Young, S., Robertson, H.M., Begovic, E., Richter, D.J., Russ, C., Westbrook, M.J., et al. (2013). Premetazoan genome evolution and the regulation of cell differentiation in the choanoflagellate Salpingoeca rosetta. Genome Biology *14*, R15.

Filmus, J., Shi, W., Wong, Z.M., and Wong, M.J. (1995). Identification of a new membrane-bound heparan sulphate proteoglycan. The Biochemical Journal *311 (Pt 2)*, 561–565.

Fuse, N., Maiti, T., Wang, B., Porter, J.A., Hall, T.M., Leahy, D.J., and Beachy, P.A. (1999). Sonic hedgehog protein signals not as a hydrolytic enzyme but as an apparent ligand for patched. Proc. Natl. Acad. Sci. U.S.A. *96*, 10992–10999.

Gish, W., and States, D.J. (1993). Identification of protein coding regions by database similarity search. Nature Genetics *3*, 266–272.

Gong, X., Qian, H., Cao, P., Zhao, X., Zhou, Q., Lei, J., and Yan, N. (2018). Structural basis for the recognition of Sonic Hedgehog by human Patched1. Science (New York, N.Y *112*, eaas8935.

González, V., Santamaría, R.I., Bustos, P., Pérez-Carrascal, O.M., Vinuesa, P., Juárez, S., Martínez-Flores, I., Cevallos, M.Á., Brom, S., Martínez-Romero, E., et al. (2019). Phylogenomic Rhizobium Species Are Structured by a Continuum of Diversity and Genomic Clusters. Front Microbiol *10*, 910.

Guo, W., and Roelink, H. (2019). Loss of the Heparan Sulfate Proteoglycan Glypican5 facilitates long-range Shh signaling. Stem Cells (Dayton, Ohio).

Hall, T.M., Porter, J.A., Beachy, P.A., and Leahy, D.J. (1995). A potential catalytic site revealed by the 1.7-A crystal structure of the amino-terminal signalling domain of Sonic hedgehog. Nature *378*, 212–216.

Hellewell, A.L., Rosini, S., and Adams, J.C. (2017). A Rapid, Scalable Method for the Isolation, Functional Study, and Analysis of Cell-derived Extracellular Matrix. J Vis Exp.

Himmelstein, D.S., Cajigas, I., Bi, C., Clark, B.S., Van Der Voort, G., and Kohtz, J.D. (2017). SHH E176/E177-Zn(2+) conformation is required for signaling at endogenous sites. Developmental Biology *424*, 221–235.

Holmquist, B., and Vallee, B.L. (1974). Metal substitutions and inhibition of thermolysin: spectra of the cobalt enzyme. J. Biol. Chem. *249*, 4601–4607.

Huang, H., Liu, S., and Kornberg, T.B. (2019). Glutamate signaling at cytoneme synapses. Science (New York, N.Y *363*, 948–955.

Incardona, J.P., Lee, J.H., Robertson, C.P., Enga, K., Kapur, R.P., and Roelink, H. (2000). Receptor-mediated endocytosis of soluble and membrane-tethered Sonic hedgehog by Patched-1. Proc. Natl. Acad. Sci. U.S.a. *97*, 12044–12049.

Lee, D.H., and Goldberg, A.L. (1996). Selective inhibitors of the proteasome-dependent and vacuolar pathways of protein degradation in Saccharomyces cerevisiae. J. Biol. Chem. *271*, 27280–27284.

Lee, J.J., Ekker, S.C., von, K.D., Porter, J.A., Sun, B.I., and Beachy, P.A. (1994). Autoproteolysis in hedgehog protein biogenesis. Science (New York, N.Y *266*, 1528–1537.

Ma, Y., Erkner, A., Gong, R., Yao, S., Taipale, J., Basler, K., and Beachy, P.A. (2002). Hedgehog-mediated patterning of the mammalian embryo requires transporter-like function of dispatched. Cell *111*, 63–75.

Macia, E., Ehrlich, M., Massol, R., Boucrot, E., Brunner, C., and Kirchhausen, T. (2006). Dynasore, a cell-permeable inhibitor of dynamin. Developmental Cell *10*, 839–850.

Matthews, B.W. (2002). Structural basis of the action of thermolysin and related zinc peptidases. Acc. Chem. Res. *21*, 333–340.

Maun, H.R., Wen, X., Lingel, A., de Sauvage, F.J., Lazarus, R.A., Scales, S.J., and Hymowitz, S.G. (2010). Hedgehog pathway antagonist 5E1 binds hedgehog at the pseudo-active site. The Journal of Biological Chemistry *285*, 26570–26580.

McCarthy, R.A., Barth, J.L., Chintalapudi, M.R., Knaak, C., and Argraves, W.S. (2002). Megalin functions as an endocytic sonic hedgehog receptor. The Journal of Biological Chemistry *277*, 25660–25667.

McLellan, J.S., Zheng, X., Hauk, G., Ghirlando, R., Beachy, P.A., and Leahy, D.J. (2008). The mode of Hedgehog binding to Ihog homologues is not conserved across different phyla. Nature *455*, 979–983.

Nüsslein-Volhard, C., and Wieshaus, E. (1980). Mutations affecting segment number and polarity in Drosophila. Nature *287*, 795–801.

Qi, X., Schmiege, P., Coutavas, E., and Li, X. (2018a). Two Patched molecules engage distinct sites on Hedgehog yielding a signaling-competent complex. Science (New York, N.Y *112*, eaas8843.

Qi, X., Schmiege, P., Coutavas, E., Wang, J., and Li, X. (2018b). Structures of human Patched and its complex with native palmitoylated sonic hedgehog. Nature *15*, 3059.

Ran, F.A., Hsu, P.D., Wright, J., Agarwala, V., Scott, D.A., and Zhang, F. (2013). Genome engineering using the CRISPR-Cas9 system. Nat Protoc *8*, 2281–2308.

Rawlings, N.D., and Barrett, A.J. (2013). Chapter 77 - Introduction: Metallopeptidases and Their Clans. In Handbook of Proteolytic Enzymes (Third Edition), N.D. Rawlings, and G. Salvesen, eds. (Academic Press), pp. 325–370.

Rebollido-Rios, R., Bandari, S., Wilms, C., Jakuschev, S., Vortkamp, A., Grobe, K., and Hoffmann, D. (2014). Signaling domain of Sonic Hedgehog as cannibalistic calcium-regulated zinc-peptidase. PLoS Comput. Biol. *10*, e1003707.

Roberts, B., Casillas, C., Alfaro, A.C., Jägers, C., and Roelink, H. (2016). Patched1 and Patched2 inhibit Smoothened non-cell autonomously. Elife *5*, e17634.

Roelink, H., Porter, J.A., Chiang, C., Tanabe, Y., Chang, D.T., Beachy, P.A., and Jessell, T.M. (1995). Floor plate and motor neuron induction by different concentrations of the amino-terminal cleavage product of sonic hedgehog autoproteolysis. Cell *81*, 445–455.

Roelink, H. (2018). Sonic Hedgehog Is a Member of the Hh/DD-Peptidase Family That Spans the Eukaryotic and Bacterial Domains of Life. Journal of Developmental Biology *6*, 12.

Roessler, E., Belloni, E., Gaudenz, K., Jay, P., Berta, P., Scherer, S.W., Tsui, L.C., and Muenke, M. (1996). Mutations in the human Sonic Hedgehog gene cause holoprosencephaly. Nature Genetics *14*, 357–360.

Siekmann, A.F., and Brand, M. (2005). Distinct tissue-specificity of three zebrafish ext1 genes encoding proteoglycan modifying enzymes and their relationship to somitic Sonic hedgehog signaling. Dev. Dyn. *232*, 498–505.

Taipale, J., Chen, J.K., Cooper, M.K., Wang, B., Mann, R.K., Milenkovic, L., Scott, M.P., and Beachy, P.A. (2000). Effects of oncogenic mutations in Smoothened and Patched can be reversed by cyclopamine. Nature *406*, 1005–9.

Taipale, J., Cooper, M.K., Maiti, T., and Beachy, P.A. (2002). Patched acts catalytically to suppress the activity of Smoothened. Nature *418*, 892–897.

Tian, H., Jeong, J., Harfe, B.D., Tabin, C.J., and McMahon, A.P. (2005). Mouse Disp1 is required in sonic hedgehog-expressing cells for paracrine activity of the cholesterol-modified ligand. Development (Cambridge, England) *132*, 133–142.

Traiffort, E., Dubourg, C., Faure, H., Rognan, D., Odent, S., Durou, M.-R., David, V., and Ruat, M. (2004). Functional characterization of sonic hedgehog mutations associated with holoprosencephaly. J. Biol. Chem. *279*, 42889–42897.

Tronrud, D.E., Roderick, S.L., and Matthews, B.W. (1992). Structural basis for the action of thermolysin. Matrix Suppl *1*, 107–111.

Tukachinsky, H., Petrov, K., Watanabe, M., and Salic, A. (2016). Mechanism of inhibition of the tumor suppressor Patched by Sonic Hedgehog. Proceedings of the National Academy of Sciences of the United States of America *113*, E5866–E5875.

van Heijenoort, J. (2011). Peptidoglycan hydrolases of Escherichia coli. Microbiol. Mol. Biol. Rev. *75*, 636–663.

Vollmer, W., and Bertsche, U. (2008). Murein (peptidoglycan) structure, architecture and biosynthesis in Escherichia coli. Biochimica Et Biophysica Acta *1778*, 1714–1734.

Waterhouse, A.M., Procter, J.B., Martin, D.M.A., Clamp, M., and Barton, G.J. (2009). Jalview Version 2--a multiple sequence alignment editor and analysis workbench. Bioinformatics *25*, 1189–1191.

Wilson, C.W., and Chuang, P.T. (2010). Mechanism and evolution of cytosolic Hedgehog signal transduction. Development (Cambridge, England) *137*, 2079–2094.

Witt, R.M., Hecht, M.-L., Pazyra-Murphy, M.F., Cohen, S.M., Noti, C., van Kuppevelt, T.H., Fuller, M., Chan, J.A., Hopwood, J.J., Seeberger, P.H., et al. (2013). Heparan sulfate proteoglycans containing a glypican 5 core and 2-O-sulfo-iduronic acid function as Sonic Hedgehog co-receptors to promote proliferation. The Journal of Biological Chemistry *288*, 26275–26288.

Sequence supplement

>Monosiga brevicollis, XP_001749037.1, 354-458
GLSFAPSSGNMYPNVVSARMASRLKVLANLVPRVFGESAAVLVLDAYRAAPLVAAEATLHNTGRAALLTVINVTASLDDELAALA
SVCADAGFDYVLYNSSAAIY

>Human, BAA33523.2, 89-193
IIFKDEENTGADRLMTQRCKDRLNSLAISVMNQWPGVKLRVTEGWDEDGHHSEESLHYEGRAVDITTSDRDRNKYGLLARLAVEA
GFDWVYYESKAHVHCSVKSE

>Mesorhizobium sp. L103C131B0, ESZ55121.1, 173-277
IVFKDEENTGADRMMTPRLKSKLDSLANVVASEWPGAKLRVTEAWDEDNEHADASLHYEGRAADLTTNPVDGAKLGRLARLAVDA
GCDWVFFEDSSHIHVSVKAG

>Micromonospora sp. HK10, WP_082159544.1, 1063-1166
IVFKDEEKTDADRMMTPRLRDMVNELAALVVKEWPGKKLRVTEGWDENNEHTAESTHYEGRAVDMTVSDLDAAKLGRLARLAVDA
GFDWVFYENALHVHASVKK

>Nematostella1 vectensis XP_001635678.1, 84-187
IVFKDEERTGADRLMSKRCREKLRNLATKVKQKWKGVKLRVTEAWDEDGQHSLDSLHYEGRAVDISTSDKDPKKLPDLGSLAVDA
GFDWVYYDRRSSIHASVRS

>Nematostella2 vectensis, ABX84114.1, 69-171
EVVFENDDCRRTTARAKSKLDVLASRVRQEWAGRKLKVIKAWTDQRTAQDPASLHYEGRALRLQLDNNDRSMLSRLAGLALASGF
DWVSYPLNSDYIHASVIRA

>Pseudoalteromonas piratica, WP_040135141.1, 60-162
PVFKFEEGNFTDVQASEKLCAAIMDLNKLVMKEWPGKTLRVTEAYDQDGEHAKFSLHNEGRAADMTVSDRDLKKLGRLGFLATKA
GFSWVYYEHNHIHASVKR

>Spirosoma aerolatum, WP_080055297.1, 211-317
VVFKNEEGDGSDRMMTPVLKTHVDRLADLVRSEWGAGVSLRVTEAWDDTGEHSSSHSLHYEGRAVDLTTSDLDKSKLGRLGRLAV
DAGFNWVYYENLLHIHASVTKA

>Varroa destructor, XP_022667503.1, 83-186
IRFLDDEGTGADRIMTQRCRDKLDTLAVSVMTQWPGVKLRVIESWDEYSHHKSGSLHYEGRAVDFTTDDRHQAKYGMLARLAVEA
GFDWVYYETKRHVHASVKP

>Drosophila melanogaster, NP_001034065.1, 144-247
ILFRDEEGTGADRLMSKRCKEKLNVLAYSVMNEWPGIRLLVTESWDEDYHHGQESLHYEGRAVTIATSDRDQSKYGMLARLAVEA
GFDWVSYVSRRHIYCSVKS

>Crocodylus porosus,XP_019386078.1, 87-190
IIFKDEENTGADRLMTQRCKDKLNALAISVMNQWPGVKLRVTEGWDEDGHHSEESLHYEGRAVDITTSDRDRSKYGMLARLAVEA
GFDWVYYESKAHIHCSVKA

>Amphimedon queenslandica, ABX90059.1, 74-180
SSQATYLHFASSDCRIMSSRLYTRLSSLAEAYYWRYHIKILVLKAWTPYPDYSLDNTSLHYEGRSVRIHVTSRNVTRLLKMAVSA
GFDWVMYDKKGYARMSVIPDAC

>Salpingoeca rosetta, XP_004997926.1, 540-646
TVKPDPPTSNGDPSVMSKRLRRHITTLASVVRGVFGDDAYVRVLEAYVEPPADISKASLHNVGRAARITIEGVPDDFASDRLGVL
GGLAVEAGFDYVAYTSRDSLYV

>Orbicella1 faveolata, XP_020616832.1, 68-170
IVFANDDCRRMTARAKSKLDVLGSRVKRQWSNAKLKVLLAWTDQIIPQAPISLHYEGRALRLQTSDGDRKKLSTLAGLAVQAGFD
WVHYATSSYIHASVIRDV

>Pocillopora1 damicornis, XP_027055961.1, 66-167
EIDFANDDCRRMTARAKSKLDVLGSTVRRQWSNVKLKVTLAWTDQIMPQAPISLHYEGRAVRLQTSDGDTGKLSTLAGLAVQAGF
DWVHYATNSYIHASVIR

>Hydra vulgaris, XP_004209904.1, 72-174
IDFQTEDSRLMTSRAKQKIDTLAGLVTTRFGKNMKVNVLKAWTDVVEKEDKLSLHYEGRAFLIRASNNDKKLLSDLMVLAREAGF
DWVYYKNEDSIYLSVIPD

>Orbicella2 faveolata, XP_020632016.1, 84-183
IIFRDEEGTGADRLMSKRCKEKLTTLAGLVKGEWPSVKLVVTEAWDEQDQHSPNSLHYEGRAVDLRLSDRDKTKIGLLGRLAVEA
GFDWVLYESRSHIHA

>Pocillopora2 damicornis, XP_027044648.1 88-190
IIFKDEEGTGADRLMSKRCQDKLNTLADLVRRQWPTVKLVVTEAWDEQGQHSENSLHYEGRAVDLRLSDKDRTKIGYLGRLAVDA
GFDWVYYQKRTHIHASVR

>Exaiptasia pallida, XP_020892909.1, 87-190
IVFKDEEGTGADRIMSKRLREKLRILAKKVKEKWRGSTRLRVIEAWDEDGTHSAHSLHYEGRAVDITTSDLDKQKYPELGRLAVE
AGFDWVFYESQEHIHASVY

>Acidobacteria bacterium, PYS76727.1, 46-149
IVFKDEEHTGDDRMMTSRLSARVDDLAARVKREFPGLKLRITEAWDDSTIHAPTSRHLEGRAVDITTSDVDHHKLGRLAGLAVEA
GFDWVFFENDLHVHASVKK

>Bacillus pseudomycoides, WP_098188151.1, 989-1092
IQFKDEEGTGADFLMTSRLSDKLNTLAILVNQEWPNIKLRVTEAWDEDNEHSSGSTHYEGRAADITTSDRDGNKLGRLAQLAVDA
GFDWVYYENKYHIHVSVKK

>Proteobacteria bacterium, PZN23661.1, 96-197
IVFKDEEATGADLLMTPRLRTRLHELARLVTREWPGVRLRVTEAWDEDSEHGENSIHYEGRAVDVTTSDRDRRKLGRLAGLAIQA
GFDWVSHERDHVHASVR

>Vogelbacteria bacterium, OHA60126.1, 199-302
ANGYSGINGPGRTDRVHRDVAEATVWVQQNLNSDHNLSTQITAAHTEGVGHSAGSEHYEGRAVDIQPTGGNVTSSNLNIIADYCR
QAGFTYVLVENRHVHCDAR

>Methylocaldum marinum, WP_119628113.1, 46-148
KSQPPIAVKKGAILAGLDRRMYFALQKARRVWSRYGKLLVVTSGLDGRHKKGSLHYVGLAVDLRSRYFAPSTRRTVTRELRRNLG
DEFQVIDEKHHIHVEFDP

>Fibrobacter sp., WP_143394061.1, 26-138
NLLIKRVQLKTGVYTGKLDAAMDSAGLVVVAEYHKVMGDSYRPTITSANDYGKHARRSKHYENKALDFRISDVPRNKRSQLVASI
RQALGKRFNVFWEEKNTANEHLHIELKE

>Chlamydia trachomatis, CRH64334.1, 1-102
MLQFKNNVRLSGVQEEILFIIDRIQRYFEVRLPKRDFVITSLTDGAHMKGSLHPKGLALDMRSRTLDKKEIEYFVTWFRKNFEKS
YDLVVEIDHIHIEYDPK

>Parcubacteria group bacterium, PSO44215.1, 232-331
ASGFRGIAGPGRTGKVKQPWVEKTKQIQEICENRYGGRPFQVTAACTYGVGHSNDSTHYRGEAVDLDPVDATNQQVISCVKEAGG
VPYYLDEDSHIHISS

>Robiginitomaculum sp., PHQ68463.1, 158-262
DENDIDIKEGADISDLTDDMTDTFDDISEAWADEAPGVTPVITSGGDGTHSTNSLHYDGNAVDLRTNNLTQAQTTTVASALSTSL
GSDYDVVVESDHIHVEYDPG

>Lentisphaerales bacterium, TFH13511.1, 91-194
WESDHDGENDEDDHLMHRGVQPLLNQLEKAVASCGAALKVHDASRPSGGGHCATSLHKEGRALDLTADGLTLEDLAKLCWVAGFD
WVFNENKRGAEHVHCSSRA

>Paraglaciecola hydrolytica, WP_068382217.1, 63-166
VVIKFEEGDCSDSKVTKNLKKTIFKLVELIDQEWEGERKLRITEAWDNNAEHTKYSLHNEGRAADITTDDRDTKKLSKLACLAMA
AGFSWVKLEKDHVHASVPR

>Rhizobium leguminosarum, WP_130783679.1, 310-413

IVFKDEEGTGADRMMSARLRDGLDRLAAQVGIEWPDVKLRVTEAWDENNEHHGASLHYEGRAADLTTSPRDGDKLGRLGKLAVDA
GLDWVFFENSAHIHVSVKR

>Verrucomicrobia bacterium, HCF95878.1, 132-232
ESDHDGDWDTENDHLVHRDILPALIRLNALVLQEGATLKIQDAYREEGIHAPASLHREGRALDLTADGMSLARLAQLAVQAGFDW
VYYESPKGGGAHIHAS

>Myxococcales bacterium, RYZ03269.1, 109-212
IVFKDEERNRSDRFMTPRLRRSLVQLSKLVSQTWPKVDLRVTEAWDDRREHGAGSVHYEGRAADITTSDQDPAKLGTLAALAVKA
GFDWVFYENATHVHVSVKR

>Branchiostoma1 floridae, XP_002599309.1, 305-414
RMLGSSLDDRCADRVMSKALLDHLRTVQRMVQDEFSGVKLKVLEAWDEPHAGATTGDHPAGSLHYEGRAAKLTLSDGDAAKLPRL
AAFCICDGAGYVENKGDHILVAVQK

>Pseudonocardia dioxanivorans, WP_103381118.1, 106-208
VVKDEEGSGADRMMTPRLAELVGVLAAHVAQAFPGRRLRLTEAWDPDGEHSHSSLHYEGRAADLTVDDRDRAKLGRLAALAVQTG
FDWVLHENDHVHVSVRAG

>Branchiostoma2 belcheri, XP_019614930.1, 311-413
DRCADRVMTKSMLDLLRKVQKMVKDEFTGVKLKVLEAWDEPHAGATEGDQPAESLHFEGRAAKLTLTDGDTSKLPQLAKNAICAG
ANFVEHKGDHIFVAVRKQ

>Acanthaster planci, XP_022111291.1, 310-422
HMKGFALNSRCADRTMSARLMATLKTLGKLVSIEWPGVKLLVLEAWDEAHEGSTYTDGDQPAGSLHYEGRAAKLSLSDGDTSKFS
RLAGLATCAAADYVEHNGDHIFVAAKKQ

>Sepia bandensis, ALM01450.1, 32-143
IVFRDEESNNEDRMMSKRCKDKLNTLAIAVMNEWPGVKLRVTEAWDTEGHHAPTSLHYEGRAVDITTSDRERSRYGMLARLAVEA
GFDWVYYESRSHIHCSVR

>Lottia gigantea, XP_009064322.1, 299-407
EKPLGNSLNQRCAARLMSQRMYNVLISLQKLVRANGDKLKVEQAFDEKYAGHVADFDATSLYTEGRLVKVTRSVNPSLANYKKLT
QWAICSKADFVQNNGDHVLIGVKK

>Crassostrea virginica, XP_022317995.1, 275-379
YPGNYLPNRCAVRVMSPRLFNVLVNLKAYASDANLGGPGGKITVEEAWDGGADPSSLRSEGRMIKVKLSAGNTAANLGKLAQLAI
CAKADHVSNMGTHLLLSVKK

>Mizuhopecten yessoensis, XP_021349176.1, 304-415
GIVGSALSKRCAARTMSYRMYKVINTLQKFVRHNMTLTDKLKVLKAWDEPYADATTGDTSYSRLHTEGRAVVVQLVSSNTASNLE
ELSHFAICAGADFISHKGDKLEIAVKK

>Bradyrhizobium sp. WSM4349, WP_018460114.1, 210-314
SIVFKDEEGTGADRMMSTRMQAKLDALASLVSAEWPGVKLRVTEAWDENDEHSPTALHYEGRAADITTQPPDGAKLGRLARLAVN
AGCDWVFYEDTNHVHVSVKK

>Paenibacillus sp. CAA11, WP_108465644.1, 1027-1131
DIVFKDEEGTGADKVMSKRMKEKLDKLAELVKKEWPSLKLRVTECWDENNEHSSNSTHYEGRGADLTTSDVDKSKLGRLGQLAVD
AGLDWVFYENDAHIHVSVKK

>Columba livia, PKK32334.1, 86-190
DIIFKDEENTGADRLMTQRCKDKLNALAISVMNQWPGVKLRVTEGWDEDGHHSEESLHYEGRAVDITTSDRDRSKYGMLARLAVE
AGFDWVYYESKAHIHCSVKA

>Ptychodera flava, BAR45718.1, 88-192
DIIFKDEEGTGADRLMTQRCKDKLNSLAILVMNQWEGIQLRVTEGWDEDGHHAENSLHYEGRAVDITTSDRDKKKYGMLARLAVQ
AGFDWVYFESKSHVHCSVRS

>Antalis entails, APD15681.1, 86-190
DVIFKDEEGTGADRMMSKTCRDKLDTLAIFVMNQWTGVKLRVTEAWDEEHHHAKDSLHYEGRAVDVTTSDRDRSKYGMLARLAVN
AGFDWVYYESRAHIHCSVNS

>Helobdella robusta, AAM70491.1, 270-374
NIIFQNSEGTGADRVMSKRCSDKLNNLASLTMEQWPGVRLRVVEAWDEDETHPEDSLHYEGRAVDVTTSDKDKSKYGMLARLAVE
AGFDWVHYEYRSHIHCSVKS

>Oryzias melastigma, ACL81248.1, 46-150
DIIFKDEENTGADRLMTQRCKDKLNSLAISVMNQWPGVKLRVTEGWDEDGHHFEESLHYEGRAVDITTSDRDKSKYGTLSRLAVE
AGFDWVYYESKAHIHCSVKA

>Trichuris suis, KFD51835.1, 95-199
NIVFKDEEGTGADRIMTNRCRYKLNLLALLVSNFWPGVKLRVIDAWEERNRQVVGSLHYEGRAVDITTSDRDNRKIPRLARLAVQ
AGFDWVYFESRQHVHASVKS

>Capitella teleta, AAZ04357.1, 82-186
DVVFKDEEGTGADRIMSQRCKDKINTLAISVMNQWPGVKLKVTEAWDEDGFHAKDSLHYEGRAVDITTDDRDRSKYGMLARLAVE
AGFDWVYYENRGHIHCSVKS

>Pipra filicauda, XP_027590561.1, 84-188
DIIFKDEENTGADRLMTQRCKDRLNSLAISVMNQWPGVKLRVTEGWDEDGHHSEESLHYEGRAVDITTSDRDRNKYGMLARLAVE
AGFDWVYYESKAHIHCSVKS

>Branchiostoma3 floridae, XP_002607850.1, 269-370
HPVGFTPSQRCADRVMSKRLYTALLRVDKHVREQLNARLRITEAWDEPHSGAADGDQAENSLHYEGRAAKLELSGSSDLTSLAKY
CICADIDYVEHKGTYLF

>Acropora millepora, XP_029199742.1, 68-170
EIDFANDDCRRMTARAKSKIDVLASRVRGRWSNVRLRVILGWTDQIPVDTQKLLHYEGRALRLQTSDRDSSKLRTLAGLAVEAGF
DWVYYASSSYIHASVIRD

>Euperipatoides kanangrensis, VDH80594.1, 88-190
IIFKDEEGTGADRLMTQRCKEKLNTLAISVMNQWPGIKLRVTEAWDEDNHHSAESLHYEGRAVDITTSDRDRSKYGMLARLAVEA
GFDWVFYESRAHIHCSVK